Biointerface Research in Applied Chemistry
Platinum Open Access Journal (ISSN: 2069-5837)

Article
Volume 11, Issue 3, 2021, 9963 - 9974
https://doi.org/10.33263/BRIAC113.99639974

A Novel Cathodic Combination in Sodium-Ion Battery Based on $NaNi_{0.7}Co_{0.3}O_2$, Na_2MnO_3, and $NaCoO_2$ Combination: Synthesis and Characterization

Samira Bagheri [1], Majid Monajjemi [2,*]

[1] Department of Chemistry, College of Science, Central Tehran Branch, Islamic Azad University, Tehran, Iran
[2] Department of Chemical Engineering, Central Tehran Branch, Islamic Azad University, Tehran, Iran
* Correspondence: maj.monajjemi@iauctb.ac.ir;

Scopus Author ID 6701810683
Received: 28.08.2020; Revised: 18.09.2020; Accepted: 20.09.2020; Published: 23.09.2020

Abstract: Several combinations, including (1-x-y) $NaNi_{0.7}Co_{0.3}O_2$, xNa_2MnO_3, and $yNaCoO_2$ systems, have been prepared by the sol-gel methods. Stoichiometric amounts of the $NaNO_3$, Mn $(Ac)_2{\cdot}4H_2O$, Co $(Ac)_2{\cdot}4H_2O$, $Ni(NO_3)_2{\cdot}\ 6H_2O$ for testing of 28 samples have been applied. We demonstrated that samples, including $Na_{1.5}Ni_{0.117}Co_{0.366}Al_{0.017}Mn_{0.5}O_2$ with Al-doped are the best composition for cathode materials in NIBTs due to the amount of cobalt (Co) in this combination, that is lower compared to $NiCoO_2$. This is important in the viewpoint of expenditure and toxic position of Co usage. Charges and discharges behavior of the cathode materials were analyzed via performing cycle tests in the range of 2.0-4.0V. Our results have shown that these kinds of samples could help to remove the unsuitable disadvantage of Co with high efficiency and also to replace Na that is cheaper instead of Li.

Keywords: sodium ion battery; $NaCoO_2$; Na_2MnO_3; sol-gel method.

1. Introduction

The cathode material elements such as manganese, nickel-cobalt (NMC), are important metals for sodium-ion batteries (NIBs) because of their abilities to operate in high voltages and large energies that can be stored in a small space. Although Ni elements give several high capacities for storing energies, they are unstable with the related electrolyte. In table 1, there are some advantages and some disadvantages items for the NMC of NIBs [1-5] comparing to NIBs. A major disadvantage of Co is its cost and toxicity, and generally, it is almost two times more costly to manufacture than the Ni. This is an important item due to any extra cost that is a basic issue. The safety factor is also a matter of crucial importance to the Na batteries that this problem appears in large size batteries as compared to the small size batteries, i.e., batteries for electric cars would have more risk of catching fire as compared to the cell phones. If a mixed solid solution is used, the explosion of batteries can be controlled, especially with doping of other elements such as Al. In addition, (1-x-y) $NaNi_{0.7}Co_{0.3}O_2$ doped with Al is suitable for the environment as compared to isolated cathode, such as $NaCoO_2$ [6-10]. The aim of this study is to find a solid ternary solution of Na-based cathode material in batteries replacement for $NaCoO_2$, which is expensive and toxic. Therefore a combination of ternary composition diagrams including (1-x-y) $NaNi_{0.7}Co_{0.3}O_2$, xNa_2MnO_3, and $yNaCoO_2$ have been investigated. NIBs were the most interesting subject among the scientist for replacing $NaCoO_2$ (reported by Rossen *et al.*). In 1992 for the NaNi0. 5Mn0. $5O_2$ [7-11]. A paper was reported in 1998 about

the electrochemical behavior that indicates Ni and Mn ions were present in "+2" and "+4" oxidation rather than the "+3". They show at a high temperature, there is a large falling capacity after 25 cycles between 100 to 155 "$mAhg^{-1}$", after 25 cycles, and to 75 "$mAhg^{-1}$" after 60 cycles. Nickel, which takes place between +2 and +4 valence positions, meanwhile manganese is +4, which remains without Jahn-Teller distortion with the +3 valance (Mn^{+3})[12-15].

Table 1. Commercial comparison between Lithium-ion battery and Sodium-ion battery.

Commercial data	**Lead-acid battery**	**LIBs**	**NIBs**
Cost	Low	High	Low
Energy Density	Low	High	Moderate/High
Safety	Moderate	Low	High
Materials	Toxic	Scarce	Earth-abundant
Cycling Stability	Moderate (high self-discharge)	High (negligible self-discharge)	High (negligible self-discharge)
Efficiency	Low (< 75%)	High (> 90%)	High (> 90%)
Temperature Range	-40 °C to 60 °C	-25 °C to 40 °C	-40 °C to 60 °C
Remarks	Mature technology; fast charging not possible	Transportation restrictions at the discharged state	Less mature technology; easy transportation

Moreover, mixing proper of various transition elements yield some advantageous efficiency of each led to the discovery of those kinds of materials. Therefore these materials are derived from Na $(Ni_{(1-x-y)}\ Mn_xCo_y)O_2$ that was published in 1999. They exhibited that the extra cobalt concentration would stabilize the composition blocks the Ni from entering the sodium layers. Meanwhile, Ni and Mn would provide structural stabilities and high capacities, respectively.

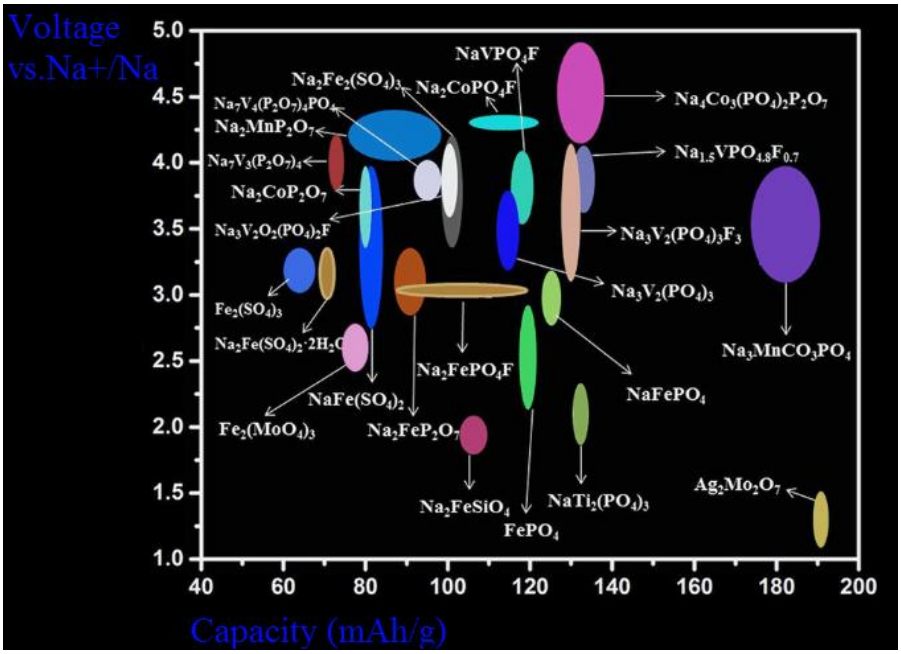

Scheme 1. Voltage-capacity diagram of various cathode materials in sodium-ion batteries

Too much of Co decrease capacities, and a large amount of Ni and Mn make problems in spinel structures; therefore, mixing of these elements must be optimized with suitable mole fraction. The layered compound of $NaNi_{1/3}Mn_{1/3}Co_{1/3}O_2$ can be synthesized and exhibited that this cathode has about 205 $mAhg^{-1}$ reversible discharge capacities in the range of 2.1-4.7 V, including large rate capabilities and thermal stabilities [16-21]. Scheme1. Voltage-Capacity curve of several cathode materials in NIB batteries for the appropriate stoichiometry of Na $(Ni_xCo_{(1-2x)}Mn_x)O_2$, x = 1/3, the medium oxidation numbers must be +3 same as Mn^{+4}, Co^{+3}, and Ni^{+2}, with the voltages in the ranges of, 2.1 up to 4.7 versus lithium ions concentration.

Moreover, about further electrochemical concepts, some extra works of $NaNi_{0.4}Mn_{0.4}Co_{0.2}O_2$, Na $(Ni_{0.8}Co_{0.2})O_2$, and $NaNi_{0.8}Co_{0.15}Al_{0.05}O_2$ cathodes have been accomplished (scheme 1). Although the rate capabilities of this material are smaller than that of $NaCoO_2$, thermal stabilities are much better [32-36]. By this work, we look at the several compositions of binary and ternary solid solutions containing Na_2MnO_3, $NacoO_2$, and (1-x-y) $NaNi_{0.7}Co_{0.3}O_2$ doped with Al (Scheme 2). Nowadays, Na_2MnO_3 has been selected for its suitable capacities, better safety, without any toxic and especially inexpensive as materials compared to $NaCoO_2$ [22-26].

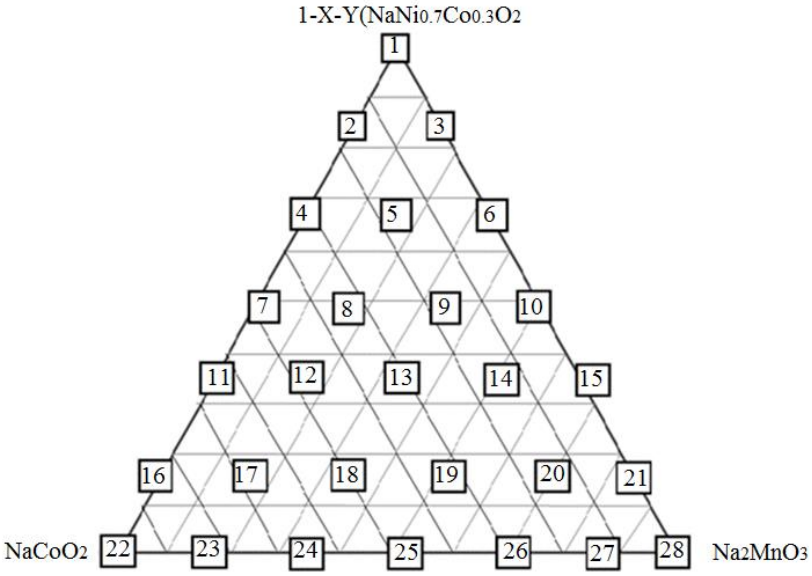

Scheme 2. Binary and Ternary diagram of {[(1-x-y) $NaNi_{0.7}Co_{0.3}O_2$] , xNa_2MnO_3 and $yNaCoO_2$ compositions.

Binary and Ternary curve of {[(1-x-y) $NaNi_{0.7}Co_{0.3}O_2$], xNa_2MnO_3, and $yNaCoO_2$ combinations, that can be denoted as Na $[Na_{1/3}Mn_{2/3}]$ O_2, have the same structure as $NaCoO_2$, except there is a super-lattice ordering of Na+ and Mn4+ in transition metal shells. Na_2MnO_3 has a rock-like layer, including Na and Mn cations in alternating (1:2 ratio, respectively) situations, and these layers are divided through a cubic O_2 layer. As Mn is shown in +4 oxidation amount, it is impossible to be further oxidization in low voltages; so Na_2MnO_3 might be electrochemically inactive, whereas these materials in higher voltages, i.e., >4.7 V, will extract the Na cation through the behind of MnO_2 shells. Meanwhile, the mechanism is unilateral and not reversible so, only one atom of Na+ ion can return during discharging towards the $NaMnO_2$ molecule. The extra Na atom that refracts within charging attaches to the higher capacities. Using of cathodes with Na_2MnO_3 is important due to simplifying the intercalation mechanism and also for providing structural stabilities during this intercalation [27-32]. Solid solutions were generally selected in terms of obtaining a cathode material with the superior capability of cycle-ability, capacities, and structural stabilities with lower costs (scheme 2).

By this work, the solid solutions have been used as a cathode material, including both binary and ternary systems. Solid solutions containing Na_2MnO_3 were found suitable for two major subjects, one the extraction of two Na+ ions at voltages > 4.7 V, where yields the extra amount of initial charges capacities, and second the MnO_2 ingredient that on the removal of Na, gives well structural stability in that combination. It is mentioned that the initial structures of the cathode material not only specified the initial characteristic capacity but also imply to the stability. The consistency of Na- dissociation cathode systems is substantial for any increase

of the cycle life. During the Na cation extracting, Ni and Co will be oxidized from +3 to +4 valance positions, so the structure cell volume will be changed. Al substitution in Co crystal is a suitable doped metal to increase stability and electrochemical efficiency. Al cation remains in the +3 valence position and has no contribution to its capacity only helps to reduce the structure volume changing and keeping the crystal stronger after a few cycling [33-39].

2. Materials and Methods

2.1. Experimental section.

The combinations were synthesized with the sol-gel method due to a simple chemical reaction, including low temperature and high homogeneity. Stoichiometric amounts of the $NaNO_3$, $Mn(Ac)_2{\cdot}4H_2O$, $Co(Ac)_2{\cdot}4H_2O$, $Ni(NO_3)_2{\cdot}6H_2O$ as starting materials of sodium, manganese, cobalt, and nickel, in 28 samples of $\{[(1\text{-}x\text{-}y)NaNi_{0.7}Co_{0.3}O_2]$ doped with Al, have been applied for several experimental testing. These mixtures were first dissolved in 50ml of DI H_2O, and then equivalence-molar weights of citric acid were added. The whole mixtures were heated via a water bath at 95ºC and during the heating process, a clear, pink solution formed. Finally, the clear solution was slowly dried and turned into gel. This solution was continuously stirred for about 30 mins for the formation of a homogeneous mixture of gel and is also kept under a hot-plate for 13-15 hrs around 95ºC. It is notable; acetate requires low and high heating temperatures to form a proper phase. The beaker containing the gel is then kept in a furnace and is heated to 460ºC for 4-6 hrs. Usually, what occurs during this stage is that whole of the acetates present would get burned off, but the desired phases are not formed. The heat-treated products were ground in an agate mortar to obtain powders, and then the powder was calcined at 850-900◦C for 11-13 hrs. The second heating is done at higher temperatures due to the wide range of materials present in the combination and also, more importantly, to ensure the formation of a correct phase for the crystalline structure then the material collected from the furnace is stored at a dry place until it is made into a cathode. The prepared products were fist mixed with acetylene black and NMP. Therefore in the system of $(1\text{-}x\text{-}y)NaNi_{0.7}Co_{0.2}Al_{0.1}$, xNa_2MnO_3, $yNaCoO_2$ (table 2), the high Ni content usually gives higher initial specific capacities while Co and Al increase the stabilities and life cycles.

3. Results and Discussion

This work (based on our previous works [40-97]) is used for explaining the best cathode material, including $(1\text{-}x\text{-}y)NaNi_{0.7}Co_{0.3}O_2$, xNa_2MnO_3, $yNaCoO_2$ systems with high initial discharge capacity, grate cyclability, and inexpensive compared to usual NIBs cathode materials. Therefore, 28 different structures using the lever rule, stoichiometric weights, and mole-fractions were selected in order to find an optimized material with suitable efficiency. These 28 points were selected via the triangle phase diagram (scheme 2 and table 2&3)and also synthesis through the sol-gel method. Ni and Al amount are decreased towards the down direction of the triangle; meanwhile, the compositions of 22, 24 have zero Ni and Al percentage. A high Mn value is found in sample 22, and its content decreases at the opposite endpoints of the triangle. Co percentage is appeared in a wide region in the triangle and also decreases near $Na(Na_{0.33}Mn_{0.66})O_2$. It is predicted which capacities and cyclability of these systems are directly related to the amount of Mn, Co, Ni, and Al. Therefore, specific capacity is determined as the number of energies which can be reserve in volume or mass (Ah), while the rate capability can be determined as the rate at which the cell is being charged.

Table 2. 28 different composition points according to using the lever rule, stoichiometric weights, and mole fractions of the triangle diagram

Sample	Composition	Al-doped
1	$NaNi_{0.7}Co_{0.3}O_2$	$NaNi_{0.7}Co_{0.2}Al_{0.1}O_2$
2	$Na_{1.167}Ni_{0.583}Co_{0.25}Mn_{0.167}O_2$	$Na_{1.167}Ni_{0.583}Co_{0.167}Al_{0.083}Mn_{0.167}O_2$
3	$NaNi_{0.583}Co_{0.417}O_2$	$NaNi_{0.583}Co_{0.334}Al_{0.083}O_2$
4	$Na_{1.333}Ni_{0.467}Co_{0.203}Mn_{0.333}O_2$	$Na_{1.333}Ni_{0.467}Co_{0.133}Al_{0.067}Mn_{0.333}O_2$
5	$Na_{1.167}Ni_{0.467}Co_{0.366}Mn_{0.167}O_2$	$Na_{1.167}Ni_{0.467}Co_{0.299}Al_{0.067}Mn_{0.167}O_2$
6	$NaNi_{0.467}Co_{0.533}O_2$	$NaNi_{0.467}Co_{0.466}Al_{0.067}O_2$
7	$Na_{1.5}Ni_{0.35}Co_{0.15}Mn_{0.5}O_2$	$Na_{1.5}Ni_{0.35}Co_{0.1}Al_{0.05}Mn_{0.5}O_2$
8	$Na_{1.333}Ni_{0.35}Co_{0.317}Mn_{0.333}O_2$	$Na_{1.333}Ni_{0.35}Co_{0.267}Al_{0.05}Mn_{0.333}O_2$
9	$Na_{1.167}Ni_{0.35}Co_{0.483}Mn_{0.167}O_2$	$Na_{1.167}Ni_{0.35}Co_{0.433}Al_{0.05}Mn_{0.167}O_2$
10	$Na\ Ni_{0.35}Co_{0.6}O_2$	$NaNi_{0.35}Co_{0.6}Al_{0.05}O_2$
11	$Na_{1.667}Ni_{0.233}Co_{0.1}Mn_{0.667}O_2$	$Na_{1.667}Ni_{0.233}Co_{0.067}Al_{0.033}Mn_{0.667}O_2$
12	$Na_{1.5}Ni_{0.233}Co_{0.267}Mn_{0.5}O_2$	$Na_{1.5}Ni_{0.233}Co_{0.234}Al_{0.033}Mn_{0.5}O_2$
13	$Na_{1.333}Ni_{0.233}Co_{0.434}Mn_{0.333}O_2$	$Na_{1.333}Ni_{0.233}Co_{0.4}Al_{0.033}Mn_{0.333}O_2$
14	$Na_{1.167}Ni_{0.233}Co_{0.6}Mn_{0.167}O_2$	$Na_{0.167}Ni_{0.233}Co_{0.567}Al_{0.033}Mn_{0.167}O_2$
15	$NaNi_{0.233}Co_{0.767}O_2$	$NaNi_{0.233}Co_{0.734}Al_{0.033}O_2$
16	$Na_{1.835}Ni_{0.116}Co_{0.049}Mn_{0.835}O_2$	$Na_{1.833}Ni_{0.117}Co_{0.033}Al_{0.017}Mn_{0.833}O_2$
17	$Na_{1.667}Ni_{0.116}Co_{0.217}Mn_{0.667}O_2$	$Na_{1.667}Ni_{0.117}Co_{0.199}Al_{0.017}Mn_{0.667}O_2$
18	$Na_{1.5}\ Ni_{0.116}Co_{0.384}Mn_{0.5}O_2$	$Na_{1.5}Ni_{0.117}Co_{0.366}Al_{0.017}Mn_{0.5}O_2$
19	$Na_{1.333}Ni_{0.116}Co_{0.551}Mn_{0.333}O_2$	$Na_{1.333}Ni_{0.117}Co_{0.533}Al_{0.017}Mn_{0.333}O_2$
20	$Na_{1.167}Ni_{0.116}Co_{0.717}Mn_{0.167}O_2$	$Na_{1.167}Ni_{0.117}Co_{0.699}Al_{0.017}Mn_{0.167}O_2$
21	$NaNi_{0.116}Co_{0.884}O_2$	$NaNi_{0.117}Co_{0.866}Al_{0.017}O_2$
22	Na_2MnO_2	Na_2MnO_2
23	$Na_{1.833}Co_{0.167}Mn_{0.833}O_2$	$Na_{1.833}Co_{0.167}Mn_{0.833}O_2$
24	$Na_{1.667}Co_{0.333}Mn_{0.667}O_2$	$Na_{1.667}Co_{0.333}Mn_{0.667}O_2$
25	$Na_{1.5}Co_{0.5}Mn_{0.5}O_2$	$Na_{1.5}Co_{0.5}Mn_{0.5}O_2$
26	$Na_{1.333}\ Co_{0.667}Mn_{0.333}O_2$	$Na_{1.333}Co_{0.667}Mn_{0.333}O_2$
27	$Na_{1.167}Co_{0.833}Mn_{0.167}O_2$	$Na_{1.167}Co_{0.833}Mn_{0.167}O_2$
28	$NaCoO_2$	$NaCoO_2$

Obviously, the C-rate is the capacity of the battery separated by the hourly charging rate. The discharge capacity diagrams have been compared with the 18650-type "C/$NaCoO_2$ Sony battery" result, which is designed by Ehrlich. Since $NaCoO_2$ cathode has an initial discharge capacity around 140 $mAhg^{-1}$, therefore any materials of these combinations with initial capacities more than this amount can be selected. The samples were tested via a cycler Arbin BT 2000 tester, in the range of 2.2 V to the 4.8 V, with a low C-rate of C/12. The initial results indicate a wide range and irregular cyclability and capacities and consequently, the initial discharge capacities varied between 100 $mAhg^{-1}$ to 250 "$mAhg^{-1}$". Both capacity and cyclability increase from $NaNi_{0.7}Co_{0.3}Al_{0.1}O_2$ towards the binary composition of Na_2MnO_3 and $NaCoO_2$.

Table 3. Summary capacity and cyclability for 28 samples of the system $[(1\text{-}x\text{-}y)NaNi_{0.7}Co_{0.2}\ Al_{0.1}]O_2$.

Sample	Blend	Na_2MnO_3	$NaCoO_2$	$NaNi_{0.7}Co_{0.2}Al_{0.1}\ O_2$	Capacity	Cyclability
1	Pure	0	0	1	80.5	61
2	Binary	0.167	0	0.833	92.3	66
3	Binary	0	0.167	0.833	99.2	85
4	Binary	0.333	0	0.667	105.5	62
5	Ternary	0.167	0.167	0.667	130.5	60
6	Binary	0	0.333	0.667	88.5	85
7	Binary	0.500	0	0.500	115.5	81
8	Ternary	0.333	0.167	0.500	107.2	61
9	Ternary	0.167	0.333	0.500	113.1	81
10	Binary	0	0.500	0.500	119.3	79
11	Binary	0.667	0	0.333	124.7	99
12	Ternary	0.500	0.167	0.333	113.1	90
13	Ternary	0.333	0.333	0.333	170.1	88
14	Ternary	0.167	0.500	0.333	163.5	85
15	Binary	0	0.667	0.333	120.6	95
16	Binary	0.833	0	0.167	171.5	65

Sample	Blend	Na_2MnO_3	$NaCoO_2$	$NaNi_{0.7}Co_{0.2}Al_{0.1}O_2$	Capacity	Cyclability
17	Ternary	0.667	0.167	0.167	131.5	91
18	Ternary	0.500	0.333	0.167	210.2*	99*
19	Ternary	0.333	0.5	0.167	119.3	92
20	Ternary	0.167	0.667	0.167	218.1	54
21	Binary	0	0.833	0.167	179.5	92
22	Pure	1	0	0	71.5	90
23	Binary	0.833	0.167	0	103.5	89
24	Binary	0.667	0.333	0	115.2	90
25	Binary	0.500	0.500	0	203.2	90
26	Binary	0.333	0.667	0	179.5	46
27	Binary	0.167	0.833	0	215.5	75
28	Pure	0	1	0	230.2	85

Although sample 20 shows a high capacity of "248.1" $mAhg^{-1}$, it contains a low cyclability. Sample 25 and 18 exhibit a good capacity of 201.2 and 220.2 $mAhg^{-1}$, respectively, with high cyclability; meanwhile because of Mn^{4+} ion, sample 22 has a low capacity.

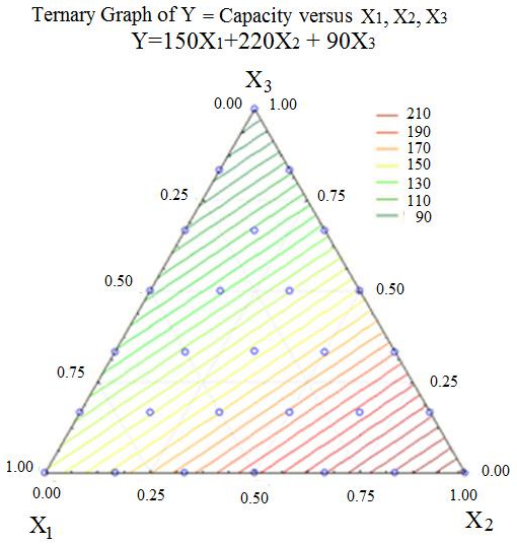

Figure 1. Ternary of capacity versus variable (1), variable (2) and variable (3) for 28 samples of (1-x-y)$NaNi_{0.7}Co_{0.2}Al_{0.1}$, xNa_2MnO_3, $yNaCoO_2$ composites.

Although this information is not enough for determining a suitable cathode material, the statistical analysis can be applied for explaining the region of the best item from the data of the 28 compositions. Therefore any testing with both capacity and cyclability relation in the viewpoint of the triangle regions is needed.

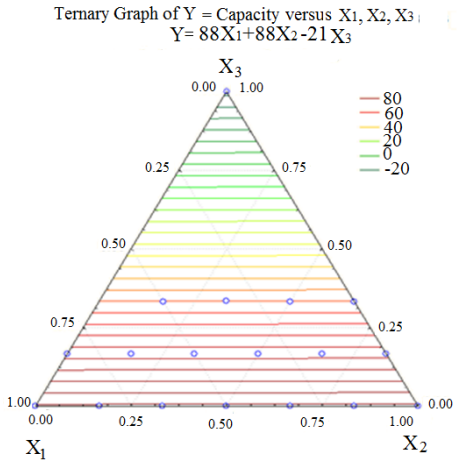

Figure 2. Ternary of cyclability versus X_1, X_2, and X_3 for 28 samples of (1-x-y)$NaNi_{0.7}Co_{0.2}Al_{0.1}$, xNa_2MnO_3, $yNaCoO_2$ composites.

In this work, the "SATISTICA" software has been selected for analyzing the data of variable (1), variable (2), and variable (3), which are Na_2MnO_3, $NaCoO_2$, and $NaNi_{0.7}Co_{0.2}Al_{0.1}O_2$ mole-fraction respectively and also the variable (4) which are capacity and cyclability alternately (table 3 and figs 1&2).

By this work, several compositions are used to explore the novel cathode materials with two-dimensional layered form through the ternary composition's diagram among Iso-structural material. Although Na_2MnO_3 or$Na[Na_{1/3}Mn_{2/3}]O_2$ has a structure similar to $NaCoO_2$, there is the super-lattice ordering of Mn^{4+} and Na^+ in transition layers. $NaNi_{0.7}Co_{0.2}Al_{0.1}O_2$ can be demonstrated as a solid solution between $NaCoO_2$ and $NaNiO_2$ with Al-doped in Co site, which is a promising cathode material due to its improved stabilities and electrochemical performances.

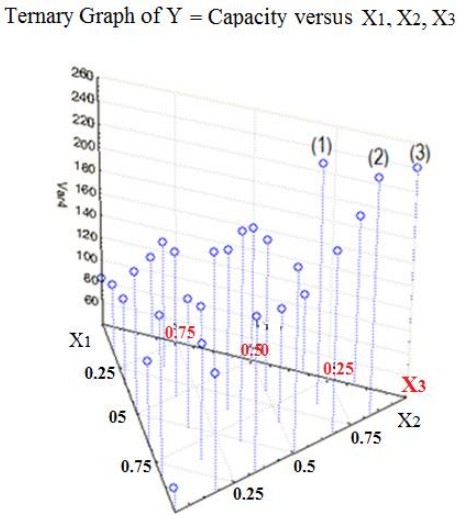

Figure 3. Three samples of (1-x-y)$NaNi_{0.7}Co_{0.2}Al_{0.1}O_2$=$X_3$, x$Na_2MnO_3$=$X_1$, y$NaCoO_2$=$X_2$ composites with high precisionist of capacity and cyclability versus X_1, X_2, and X_3.

With more testing, three samples were chosen and subsequently synthesized, characterized, and tested consequently with high precisionists. Via initial discharge capacity and some other information, numbers 18, 27, and 28 are indicated as the best cathode material among those structures (figs. 3&4, table 2&3). As the number 28 is pure material ($NaCoO_2$), and number 27 is binary, the number 18 "$Na_{1.5}Ni_{0.117}Co_{0.366}Al_{0.017}Mn_{0.5}O_2$" is suggested as the best combination for cathode material.

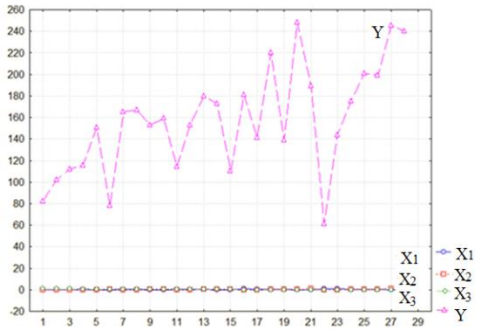

Figure 4. Multiple variable combinations of capacities and cyclability are based on the mole-fraction of X_1,X_2, and X_3 in 28 compositions.

The repeat of sample 20 was made into T-Cells and subjected to electrochemical testing using the original conditions, and the cycling was done between 2.1-4.7 V with constant C-rate of C/12 at room temperature (fig. 5). The repeated sample shows suitable charge and discharge capacities (discharge capacity of 150, $mAhg^{-1}$) than the original sample. With the same method,

we used (1-x-y)$NaNi_{0.7}Co_{0.3}O_2$, xNa_2MnO_3, and $yNaCoO_2$ composites; the sample $Na_{1.5}Ni_{0.117}Co_{0.366}Al_{0.017}Mn_{0.5}O_2$ has been tested for comparing in viewpoints of capacity and cyclability (Fig. 5), the repeat sample exhibits in the same mole fraction, the system with Al-doped has a better charge, and discharge capacities (discharge capacity of 155, $mAhg^{-1}$) compared to the non-Al-doped system (discharge capacity of 144, $mAhg^{-1}$).

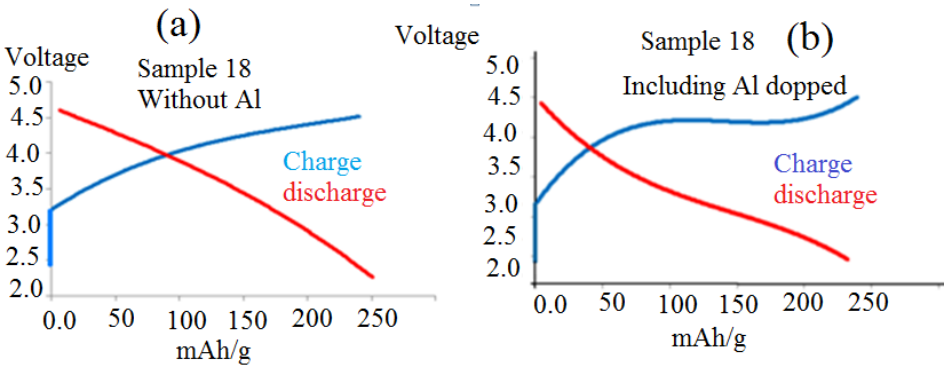

Figure 5. Charge and discharge capacity of (a): $Na_{1.5}$ $Ni_{0.116}Co_{0.384}Mn_{0.5}O_2$ and (b): $Na_{1.5}Ni_{0.117}$ $Co_{0.366}$ $Al_{0.017}$ $Mn_{0.5}O_2$.

4. Conclusions

[(1-x-y)$NaNi_{0.7}Co_{0.3}O_2$] doped with Al for cathode materials have been successfully synthesized via a sol-gel method. The results show that all the prepared "$Na_{1.5}Ni_{0.117}Co_{0.366}Al_{0.017}Mn_{0.5}O_2$" type layered structure of the nickel content and Al-doped improve the capacity retention significantly. The percentage of Ni and Co exhibits good efficiency. Although these kinds of systems can help to remove the disadvantage of Co, the efficiency of these kind systems is similar to $NaCoO_2$ cathode material. Therefore, the fabrication of Sodium-ion batteries using a few more transition elements such as Mn and Al are suggested for any further research.

Funding

This research was funded by ourselves.

Acknowledgments

Thanks to the Central Tehran Branch, Islamic Azad University for supporting computational software and all necessary equipment.

Conflicts of Interest

The authors declare no conflict of interest.

References

1. Cheng, F.; Liang, J.; Tao, Z.; Chen, J. Functional materials for rechargeable batteries. *Advanced Materials* **2011,** *23*, 1695-1715, https://doi.org/10.1002/adma.201003587.
2. Whittingham, M.S. Materials challenges facing electrical energy storage. *MRS Bulletin* **2008,** *33*, 411-419, https://doi.org/10.1557/mrs2008.82.
3. She-Huang, W.; Su, H.S. Electrochemical characteristics of partially cobalt-substituted LiMn2-*y*Co*y*O4 spinels synthesized by Pechini process. *Materials Chemistry and Physics* **2002**, *78*, 189–195, https://doi.org/10.1016/S0254-0584(02)00346-2.
4. Tarascon, J.M.; Armand, M. Issues and challenges facing rechargeable lithium batteries. *Nature* **2001,** *414*, 359-367, https://doi.org/10.1038/35104644.

5. Nagaura, T.T.K. Lithium ion recheargable battery. *Progress in Batteries & Solar Cells***. 1990,** *9*.
6. Scrosati, B.; Garche, J. Lithium batteries: Status, prospects and future. *Journal of Power Sources* **2010,** *195*, 2419-2430, https://doi.org/10.1016/j.jpowsour.2009.11.048.
7. Whittingham, M.S. Lithium Batteries and Cathode Materials. *Chemical Reviews* **2004**, *104*, 4271-4302, https://doi.org/10.1021/cr020731c.
8. Bruce, P.G.; Scrosati, B.; Tarascon, J.M. Nanomaterials for Rechargeable Lithium Batteries. *Angewandte Chemie International Edition* **2008,** *47*, 2930-2946, https://doi.org/10.1002/anie.200702505.
9. Goodenough, J.B.; Kim, Y. Challenges for Rechargeable Li Batteries. *Chemistry of Materials* **2009,** *22*, 587-603, https://doi.org/10.1021/cm901452z.
10. Kaskhedikar, N.A.; Maier, J. Lithium storage in carbon nanostructures. *Advanced Materials* **2009,** *21*, 2664-2680, https://doi.org/10.1002/adma.200901079.
11. Cabana, J.; Monconduit, L.; Larcher, D.; Palacin, M.R. Beyond intercalation-based Liion batteries: The state of the art and challenges of electrode materials reacting through conversion reactions. *Advanced Materials* **2010,** *22*, 170-192, https://doi.org/10.1002/adma.201000717.
12. Poizot, P.; Laruelle, S.; Grugeon, S.; Dupont, L.; Tarascon, J.M. Nano-sized transition-metaloxides as negative-electrode materials for lithium-ion batteries. *Nature* **2000,** *407*, 496-499, https://doi.org/10.1038/35035045.
13. Park, J.C.; Kim, J.; Kwon, H.; Song, H. Gram-Scale Synthesis of Cu2O Nanocubes and Subsequent Oxidation to CuO Hollow Nanostructures for Lithium-Ion Battery Anode Materials. *Advanced Materials* **2009,** *21*, https://doi.org/10.1002/adma.200800596.
14. Ban, C.M., Wu, Z.C.; Gillaspie, D.T.; Chen, L.; Yan, Y.F.; Blackburn, J.L.; Dillon, A.C. Nanostructured Fe_3O_4/SWNT Electrode: Binder-Free and High-Rate Li-Ion Anode**.** *Advanced Materials* **2010,** *22*, https://doi.org/10.1002/adma.200904285.
15. Doh, C.H.; Kalaiselvi, N.; Park, C.W.; Jin, B.S.; Moon, S.I.; Yun, M.S. Synthesis and electrochemical characterization of novel high capacity Si3-xFexN4 anode for rechargeable lithium batteries. *Electrochemistry Communications* **2004,** *6*, 965-968, https://doi.org/10.1016/j.elecom.2004.07.011.
16. Cabana, J.; Stoeva, Z.; Titman, J.J.; Gregory, D.H.; Palacin, M.R. Towards new negative electrode materials for Li-ion batteries: Electrochemical properties of Li-Ni-N. *Chemistry of Materials* **2008,** *20*, 1676-1678, https://doi.org/10.1021/cm7034486.
17. Morgan, D.; Van der Ven, A.; Ceder, G. Li conductivity in LixMPO4 (M = Mn, Fe, Co, Ni) olivine aterials. *Electrochemical and Solid State Letters* **2004,** *7*, 30-32.
18. Muraliganth, T.; Murugan, A.V.; Manthiram, A. Nano scale networking of LiFePO4 nano rods synthesized by a microwavesolvo thermal route with carbon nanotubes for lithium ion batteries. *Journal of Materials Chemistry* **2008,** *18*, 5661-5668, http://dx.doi.org/10.1039/b812165f.
19. Yamada, A.; Chung, S.C.; Hinokuma, K. Optimized LiFePO4 for lithium battery cathodes. *Journal of the Electrochemical Society* **2001,** *148*, 224-229.
20. Wang, Y.G.; Wang, Y.R.; Hosono, E.J.; Wang, K X.; Zhou, H.S. The design of a LiFePO4/carbon nano-composite with a core-shell structure and its synthesis by an in situ polymerization restriction method. *Angewandte Chemie-International Edition* **2008,** *47*, 7461-7465, https://doi.org/10.1002/anie.200802539**.**
21. Zhou, Y.; Wang, J.; Hu, Y.; O'Hayre, R.; Shao, Z. A porous LiFePO4 and carbon nanotube composite. *Chemical Communications* **2010,** *46*, 7151-7153, https://doi.org/10.1039/C0CC01721C.
22. Liu, J.; Conry, T.E.; Song, X.; Doeff , M.M.; Richardson, T.J. Nano-porous spherical LiFePO4 for high performance cathodes. *Energy & Environmental Science* **2011,** *4*, 885-888, https://doi.org/10.1039/c0ee00662a.
23. Saravanan, K.; Balaya, P.; Reddy, M.V.; Chowdari, B.V.R.; Vittal, J.J. Morphology controlled synthesis of LiFePO4/C nano plates for Li-ion batteries. *Energy & Environmental Science* **2010,** *3*, 457-464**,** https://doi.org/10.1039/B923576K.
24. Srinivasan, V.; Newman, J. Discharge model for the lithium iron-phosphate electrode. *Journal of the Electrochemical Society* **2004,** *151*, 1517-1529.
25. Akimoto, J.; Gotoh, Y.; Oosawa, Y. Synthesis and Structure Refinement of LiCoO2 Single Crystals. *Journal of Solid State Chemistry* **1998**, *141*, 298-302.
26. Madhu, C.; Garrett, J.; Manivannan, V. Synthesis and characterization of oxide cathode materials of the system (1- y)LiNiOxLiMnOyLiC oO. *Ionics* **2010**, *16*, 591-602.
27. Sun, Y. The preparation and electrochemical performance of solid solutions LiCoO2–Li2MnO3 as cathode materials for lithium ion batteries. *Journal of Power Sources* **2006**, *159*, 1353-1359, https://doi.org/10.1016/j.jpowsour.2005.12.037.
28. Jiang, J. Structure, Electrochemical Properties, and Thermal Stability Studies of Cathode Materials in the xLi [Mn 1/2] NiOy LiCoOzLi [Li1/3] Mn[2/3] O2 Pseudoternary System (x + y + z = 1). *Journal of The Electrochemical Society* **2005**, *152*, 1879-1889.
29. Zhong, Q. Synthesis and Electrochemistry of LiNiMn- xO2. *Journal of the Electro -chemical Society*. **1997**, *144*, 205-213. 30.

30. Zhong, S.W.; Zhao, Y.J.; Li, Y.; Li, P.Z.; Mei, J.; Liu, Q.G. Characteristics and electrochemical performance of cathode material Co coated LiNiO2 for Li-ion batteries. *Transactions of Nonferrous Metals Society of China* **2006**, *16*, 137-141, https://doi.org/10.1016/S1003-6326(06)60024-1.
31. Amatucci, G.; Pasquier, A.D.; Blyr, A.; Zheng, T.; Tarascon, J.M. The elevated temperature performance of the LiMn2O4/C system: failure and solutions. *Electrochimica Acta* **1999,** *45*, 255-271, https://doi.org/10.1016/S0013-4686(99)00209-1.
32. Liu, L.; Wang, Z.; Li, H.; Chen, L.; Huang, X. Al2O3-coated LiCoO2 as cathode material for lithium ion batteries. *Solid State Ionics* **2002**, *152*, 341-346, https://doi.org/10.1016/S0167-2738(02)00333-8.
33. Mikhaylik, Y.V.; Akridge, J.R. Low Temperature Performance of Li/S Batteries. *J. Electrochem. Soc.* **2003**, *150*, 306.
34. Colfen, H.; Mann, S. Higher-order organization by mesoscale self-assembly and transformation of hybrid nanostructures. *Angewandte Chemie-International Edition* **2003,** *42*, 2350-2365, https://doi.org/10.1002/anie.200200562.
35. Colfen, H.; Antonietti, M. Mesocrystals: Inorganic superstructures made by highly parallel crystallization and controlled alignment. *Angewandte Chemie-International Edition* **2005**, *44*, 5576-5591, https://doi.org/10.1002/anie.200500496.
36. Yu, S.H.; Colfen, H.; Tauer, K.; Antonietti M. Tectonic arrangement of BaCO3 nanocrystals into helices induced by a racemic block copolymer. *Nature Materials* **2005,** *4*, 51-55, https://doi.org/10.1038/nmat1268.
37. Song, R.Q.; Colfen, H. Mesocrystals-ordered nanoparticle superstructures. *Advanced Materials* **2010,** *22*, 1301-1330, https://doi.org/10.1002/adma.200901365.
38. Colfen, H.; Antonietti, M. *Mesocrystals and nonclassical crystallization*. John Wiley & Sons, Ltd, **2008**; https://doi.org/10.1002/9780470994603.
39. Kanamura, K.; Koizumi, S.H.; Dokko, K.R. Hydrothermal synthesis of LiFePO4 as a cathode material for lithium batteries. *Journal of Materials Science* **2008**, *43*, 2138-2142, http://dx.doi.org/10.1007/s10853-007-2011-1.
40. Mollaamin, F.; Monajjemi, M. DFT outlook of solvent effect on function of nano bioorganic drugs. *Physics and Chemistry of Liquids* **2012**, *50*, 596-604, https://doi.org/10.1080/00319104.2011.646444.
41. Mollaamin, F.; Gharibe, S.; Monajjemi, M. Synthesis of various nano and micro ZnSe morphologies by using hydrothermal method. *International Journal of Physical Sciences* **2011**, *6*, 1496-1500.
42. Monajjemi, M. Graphene/(h-BN)*n*/X-doped raphene as anode material in lithium ion batteries (X = Li, Be, B AND N,). *Macedonian Journal of Chemistry and Chemical Engineering* **2017**, *36*, 101–118, http://dx.doi.org/10.20450/mjcce.2017.1134.
43. Monajjemi, M. Cell membrane causes the lipid bilayers to behave as variable capacitors: A resonance with self-induction of helical proteins. *Biophysical Chemistry* **2015**, *207*, 114-127, https://doi.org/10.1016/j.bpc.2015.10.003.
44. Monajjemi, M. Study of CD5+ Ions and Deuterated Variants (CHxD(5-x)+): An Artefactual Rotation. *Russian Journal of Physical Chemistry A* **2018,** *92***,** 2215-2226.
45. Monajjemi, M. Liquid-phase exfoliation (LPE) of graphite towards graphene: An ab initio study. *Journal of Molecular Liquids*, **2017**, *230*, 461–472, https://doi.org/10.1016/j.molliq.2017.01.044.
46. Jalilian, H.; Monajjemi, M. Capacitor simulation including of X-doped graphene (X = Li, Be, B) as twoelectrodes and (h-BN)m (m = 1–4) as the insulator. *Japanese Journal of Applied Physics* **2015**, *54*, 085101-7.
47. Ardalan, T.; Ardalan, P.; Monajjemi, M. Nano theoretical study of a C 16 cluster as a novel material for vitamin C carrier. *Fullerenes Nanotubes and Carbon Nanostructures* **2014**, *22*, 687-708, https://doi.org/10.1080/1536383X.2012.717561.
48. Mahdavian, L.; Monajjemi, M.; Mangkorntong, N. Sensor response to alcohol and chemical mechanism of carbon nanotube gas sensors *Fullerenes Nanotubes and Carbon Nanostructures* **2009**, *17*, 484-495, https://doi.org/10.1080/15363830903130044.
49. Monajjemi, M.; Najafpour, J. Charge density discrepancy between NBO and QTAIM in single-wall armchair carbon nanotubes. *Fullerenes Nanotubes and Carbon Nano structures* **2014**, *22*, 575-594, https://doi.org/10.1080/1536383X.2012.702161.
50. Monajjemi, M.; Hosseini, M.S. Non bonded interaction of B16 N16 nano ring with copper cations in point of crystal fields. *Journal of Computational and Theoretical Nanoscience* **2013**, *10*, 2473-2477.
51. Monajjemi, M.; Mahdavian, L.; Mollaamin, F. Characterization of nanocrystalline silicon germanium film and nanotube in adsorption gas by Monte Carlo and Langevin dynamic simulation. *Bulletin of the Chemical Society of Ethiopia* **2008**, *22*, 277-286, https://doi.org/10.4314/bcse.v22i2.61299.
52. Lee, V.S.; Nimmanpipug, P.; Mollaamin, F.; Thanasanvorakun, S.; Monajjemi, M. Investigation of single wall carbon nanotubes electrical properties and normal mode analysis: Dielectric effects. *Russian Journal of Physical Chemistry A* **2009**, *83*, 2288-2296, https://doi.org/10.1134/S0036024409130184.
53. Mollaamin, F.; Najafpour, J.; Ghadami, S.; Akrami, M.S.; Monajjemi, M. The electromagnetic feature of B N H (x = 0, 4, 8, 12, 16, and 20) nano rings:Quantum theory of atoms in molecules/NMR approach. *Journal of Computational and Theoretical Nanoscience* **2014**, *11*, 1290-1298.

54. Monajjemi, M.; Mahdavian, L.; Mollaamin, F.; Honarparvar, B. Thermodynamic investigation of enolketo tautomerism for alcohol sensors based on carbon nanotubes as chemical sensors. *Fullerenes Nanotubes and Carbon Nanostructures* **2010**, *18*, 45-55, https://doi.org/10.1080/15363830903291564.
55. Monajjemi, M.; Ghiasi, R.; Seyed, S.M.A. Metal-stabilized rare tautomers: N4 metalated cytosine (M = Li , Na , K , Rb and Cs), theoretical views. *Applied Organometallic Chemistry* **2003**, *17*, 635-640, https://doi.org/10.1002/aoc.469.
56. Ilkhani, A.R.; Monajjemi, M. The pseudo Jahn-Teller effect of puckering in pentatomic unsaturated rings C AE , A=N, P, As, E=H, F, Cl.*Computational and Theoretical Chemistry* **2015**, *1074*, 19-25, http://dx.doi.org/10.1016%2Fj.comptc.2015.10.006.
57. Monajjemi, M. Non-covalent attraction of B N and repulsion of B N in the B N ring: a quantum rotatory due to an external field. *Theoretical Chemistry Accounts* **2015**, *134*, 1-22, https://doi.org/10.1007/s00214-015-1668-9.
58. Monajjemi, M.; Naderi, F.; Mollaamin, F.; Khaleghian, M. Drug design outlook by calculation of second virial coefficient as a nano study. *Journal of the Mexican Chemical Society* **2012**, *56*, 207-211, https://doi.org/10.29356/jmcs.v56i2.323.
59. Monajjemi, M.; Bagheri, S.; Moosavi, M.S. Symmetry breaking of B2N(-,0,+): An aspect of the electric potential and atomic charges. *Molecules* **2015**, *20*, 21636-21657, https://doi.org/10.3390/molecules201219769.
60. Monajjemi, M.; Mohammadian, N.T. S-NICS: An aromaticity criterion for nano molecules. *Journal of Computational and Theoretical Nanoscience* **2015**, *12*, 4895-4914, https://doi.org/10.1166/jctn.2015.4458.
61. Monajjemi, M.; Ketabi, S.; Hashemian, Z.M.; Amiri, A. Simulation of DNA bases in water: Comparison of the Monte Carlo algorithm with molecular mechanics force fields. *Biochemistry (Moscow)* **2006**, *71*, 1-8, https://doi.org/10.1134/s0006297906130013.
62. Monajjemi, M.; Lee, V.S.; Khaleghian, M.; Honarparvar, B.; Mollaamin, F. Theoretical Description of Electromagnetic Nonbonded Interactions of Radical, Cationic, and Anionic NH2BHNBHNH2 Inside of the B18N18 Nanoring. *J. Phys. Chem C* **2010**, *114*, 15315-15330, https://doi.org/10.1021/jp104274z.
63. Monajjemi, M.; Boggs, J.E. A New Generation of BnNn Rings as a Supplement to Boron Nitride Tubes and Cages. *J. Phys. Chem. A* **2013**, *117*, 1670-1684, http://dx.doi.org/10.1021/jp312073q.
64. Monajjemi, M.; Robert, W.J.; Boggs, J.E. NMR contour maps as a new parameter of carboxyl's OH groups in amino acids recognition: A reason of tRNA–amino acid conjugation. *Chemical Physics* **2014**, *433*, 1-11, https://doi.org/10.1016/j.chemphys.2014.01.017.
65. Monajjemi, M. Quantum investigation of non-bonded interaction between the B15N15 ring and BH2NBH2 (radical, cation, and anion) systems: a nano molecularmotor. *Struct Chem* **2012,** *23*, 551–580, http://dx.doi.org/10.1007/s11224-011-9895-8.
66. Monajjemi, M. Metal-doped graphene layers composed with boron nitride–graphene as an insulator: a nanocapacitor. *Journal of Molecular Modeling* **2014**, *20*, https://doi.org/10.1007/s00894-014-2507-y.
67. Mollaamin, F.; Monajjemi, M.; Mehrzad, J. Molecular Modeling Investigation of an Anti-cancer Agent Joint to SWCNT Using Theoretical Methods. *Fullerenes, Nanotubes and Carbon Nanostructures* **2014**, *22*, 738-751, https://doi.org/10.1080/1536383X.2012.731582.
68. Monajjemi, M.; Ketabi, S.; Amiri, A. Monte Carlo simulation study of melittin: protein folding and temperature ependence. *Russian journal of physical chemistry* **2006**, *80*, S55-S62, https://doi.org/10.1134/S0036024406130103.
69. Monajjemi, M.; Heshmata, M.; Haeria, H.H. QM/MM model study on properties and structure of some antibiotics in gas phase: Comparison of energy and NMR chemical shift. *Biochemistry (Moscow)* **2006**, *71*, S113-S122, https://doi.org/10.1134/S0006297906130190.
70. Monajjemi, M.; Afsharnezhad, S.; Jaafari, M.R.; Abdolahi, T.; Nikosade, A.; Monajemi, H. NMR shielding and a thermodynamic study of the effect of environmental exposure to petrochemical solvent on DPPC, an important component of lung surfactant. *Russian Journal of Physical Chemistry A* **2007**, *81*, 1956-1963, https://doi.org/10.1134/S0036024407120096.
71. Mollaamin, F.; Noei, M.; Monajjemi, M.; Rasoolzadeh, R. Nano theoretical studies of fMET-tRNA structuren in protein synthesis of prokaryotes and its comparison with the structure of fALA-tRNA. *Africanjournal of microbiology research* **2011**, *5*, 2667-2674, https://doi.org/10.5897/AJMR11.310.
72. Monajjemi, M.; Heshmat, M.; Haeri, H.H.; Kaveh, F. Theoretical study of vitamin properties from combined QM-MM methods: Comparison of chemical shifts and energy. *Russian Journal of Physical Chemistry* **2006**, *80*, 1061-1068, https://doi.org/10.1134/S0036024406070119.
73. Monajjemi, M.; Chahkandi, B. Theoretical investigation of hydrogen bonding in Watson–Crick, Hoogestein and their reversed and other models: comparison and analysis for configurations of adenine–thymine base pairs in 9 models. *Journal of Molecular Structure: Theochem* **2005**, *714*, 43-60, https://doi.org/10.1016/j.theochem.2004.09.048.
74. Monajjemi, M.; Honarparvar, B.; Haeri, H.H.; Heshmat, M. An ab initio quantum chemical investigation of solvent-induced effect on 14N-NQR parameters of alanine, glycine, valine, and serine using a polarizable continuum model. *Russian Journal of Physical Chemistry* **2006**, *80*, S40-S44, https://doi.org/10.1134/S0036024406130073.

75. Monajjemi, M.; Seyed Hosseini, M. Non Bonded Interaction of B16N16 Nano Ring with Copper Cations in Point of Crystal Fields. *Journal of Computational and Theoretical Nanoscience* **2013**, *10*, 2473-2477, https://doi.org/10.1166/jctn.2013.3233.
76. Monajjemi, M.; Farahani, N.; Mollaamin, F. Thermodynamic study of solvent effects on nanostructures: phosphatidylserine and phosphatidylinositol membranes. *Physics and Chemistry of Liquids* **2012**, *50*, 161-172, https://doi.org/10.1080/00319104.2010.527842.
77. Monajjemi, M.; Ahmadianarog, M. Carbon Nanotube as a Deliver for Sulforaphane in Broccoli Vegetable in Point of Nuclear Magnetic Resonance and Natural Bond Orbital Specifications. *Journal of Computational and Theoretical Nanoscience* **2014**, *11*, 1465-1471, https://doi.org/10.1166/jctn.2014.3519.
78. Monajjemi, M.; Ghiasi, R.; Ketabi, S.; Passdar, H.; Mollaamin, F. A Theoretical Study of Metal-Stabilised Rare Tautomers Stability: N4 Metalated Cytosine (M=Be2+, Mg2+, Ca2+, Sr2+ and Ba2+) in Gas Phase and Different. *Journal of Chemical Research* **2004**, *1*, 11-18, https://doi.org/10.3184/030823404323000648.
79. Monajjemi, M.; Baei, M.T.; Mollaamin, F. Quantum mechanic study of hydrogen chemisorptions on nanocluster vanadium surface. *Russian Journal of Inorganic Chemistry* **2008**, *53*, 1430-1437, https://doi.org/10.1134/S0036023608090143.
80. Mollaamin, F.; Baei, M.T.; Monajjemi, M.; Zhiani, R.; Honarparvar, B. A DFT study of hydrogen chemisorption on V (100) surfaces. *Russian Journal of Physical Chemistry A, Focus on Chemistry* **2008**, *82*, 2354-2361, https://doi.org/10.1134/S0036024408130323 .
81. Monajjemi, M.; Honarparvar, B.; Nasseri, S.M.; Khaleghian, M. NQR and NMR study of hydrogen bonding interactions in anhydrous and monohydrated guanine cluster model: A computational study. *Journal of Structural Chemistry* **2009**, *50*, 67-77, https://doi.org/10.1007/s10947-009-0009-z.
82. Monajjemi, M.; Aghaie, H.; Naderi, F. Thermodynamic study of interaction of TSPP, CoTsPc, and FeTsPc with calf thymus DNA. *Biochemistry (Moscow)* **2007**, *72*, 652-657, https://doi.org/10.1134/S0006297907060089.
83. Monajjemi, M.; Heshmat, M.; Aghaei, H.; Ahmadi, R.; Zare, K. Solvent effect on 14N NMR shielding of glycine, serine, leucine, and threonine: Comparison between chemical shifts and energy versus dielectric constant. *Bulletin of the Chemical Society of Ethiopia* **2007**, *21*, 111-116, https://doi.org/10.4314/bcse.v21i1.61387.
84. Monajjemi, M.; Rajaeian, E.; Mollaamin, F.; Naderi, F.; Saki, S. Investigation of NMR shielding tensors in 1,3 dipolar cycloadditions: solvents dielectric effect. *Physics and Chemistry of Liquids* **2008**, *46*, 299-306, https://doi.org/10.1080/00319100601124369.
85. Mollaamin, F.; Varmaghani, Z.; Monajjemi, M. Dielectric effect on thermodynamic properties in vinblastine by DFT/Onsager modelling. *Physics and Chemistry of Liquids* **2011**, *49*, 318-336, https://doi.org/10.1080/00319100903456121.
86. Monajjemi, M.; Honaparvar, B.; Khalili Hadad, B.; Ilkhani, A.; Mollaamin, F. Thermo-Chemical Investigation and NBO Analysis of Some anxileotic as Nano- Drugs. *African journal of pharmacy and pharmacology* **2010**, *4*, 521-529.
87. Monajjemi, M.; Khaleghian, M.; Mollaamin, F. Theoretical study of the intermolecular potential energy and second virial coefficient in the mixtures of CH4 and Kr gases: a comparison with experimental data. *Molecular Simulation* **2010**, *36*, 865-870, https://doi.org/10.1080/08927022.2010.489557.
88. Monajjemi, M.; Khosravi, M.; Honarparvar, B.; Mollaamin, F. Substituent and solvent effects on the structural bioactivity and anticancer characteristic of catechin as a bioactive constituent of green tea. *International Journal of Quantum Chemistry* **2011**, *111*, 2771-2777, https://doi.org/10.1002/qua.22612.
89. Tahan, A.; Monajjemi, M. Solvent dielectric effect and side chain mutation on the structural stability of Burkholderia cepacia lipase active site: a quantum mechanical/molecular mechanics study. *Acta Biotheor* **2011**, *59*, 291-312, https://doi.org/10.1007/s10441-011-9137-x.
90. Monajjemi, M.; Khaleghian, M. EPR Study of Electronic Structure of [CoF6]3-and B18N18 Nano Ring Field Effects on Octahedral Complex. *Journal of Cluster Science* **2011**, *22*, 673-692, https://doi.org/10.1007/s10876-011-0414-2.
91. Monajjemi, M.; Mollaamin, F. Molecular Modeling Study of Drug-DNA Combined to Single Walled Carbon Nanotube. *Journal of Cluster Science* **2012**, *23*, 259-272, https://doi.org/10.1007/s10876-011-0426-y.
92. Mollaamin, F.; Monajjemi, M. Fractal Dimension on Carbon Nanotube-Polymer Composite Materials Using Percolation Theory. *Journal of Computational and Theoretical Nanoscience* **2012**, *9*, 597-601, https://doi.org/10.1166/jctn.2012.2067.
93. Mahdavian, L.; Monajjemi, M. Alcohol sensors based on SWNT as chemical sensors: Monte Carlo and Langevin dynamics simulation. *Microelectronics Journal* **2010**, *41*, 142-149, https://doi.org/10.1016/j.mejo.2010.01.011.
94. Monajjemi, M.; Falahati, M.; Mollaamin, F. Computational investigation on alcohol nanosensors in combination with carbon nanotube: a Monte Carlo and ab initio simulation. *Ionics* **2013**, *19*, 155-164, https://doi.org/10.1007/s11581-012-0708-x.
95. Monajjemi, M. Non bonded interaction between BnNn (stator) and BN B (rotor) systems: A quantum rotation in IR region. *Chemical Physics* **2013**, *425*, 29-45, https://doi.org/10.1016/j.chemphys.2013.07.014.